Military Technical College
Kobry El-Kobbah,
Cairo, Egypt

14th International Conference on Applied Mechanics and Mechanical Engineering.

Modeling of the Gas and Particle Flow in the Cyclone Separator using LES, RANS and Mathematical Models

By

Kh. Elsayed* C. Lacor**

Abstract:

The numerical simulation of the fluid flow and particle dynamics is presented by CFD simulations based on Navier-Stokes equations with the Reynolds stress turbulence model (RSM) and large eddy simulation (LES). A Lagrangian method is employed to track the particle motion and calculate the gas - particle separation efficiency in the cyclones for RSM and LES. According to the computational results, the differences of pressure, velocity and turbulence parameters of the gas flow are described to address the effects of the turbulence methodology on the obtained flow pattern of cyclones, especially for the tangential and axial velocity distributions. A comparison of experimental data, CFD simulation and different mathematical models has been performed to estimate the suitability of the three methodologies for estimation of cyclone performance and flow field. The results indicate that, the CFD approach can effectively reveal the mechanisms of gas-particle flow and separation in cyclones via RSM and LES, with overestimating of LES especially for pressure drop. Also a good matching is obtained from mathematical models for the cyclone pressure drop and cut-off size.

Keywords:

Cyclone separator, Reynolds stress model (RSM), Large eddy simulation (LES), Discrete phase modeling (DPM), One-Way coupling, Mathematical models.

---

* PhD researcher, Department of Mechanical Engineering, Vrije Universiteit Brussel, Pleinlaan 2 -1050 Brussels- Belgium, Email: khairy.elsayed@vub.ac.be.
** Professor, Department of Mechanical Engineering, Vrije Universiteit Brussel, Pleinlaan 2 -1050 Brussels- Belgium, Email: chris.lacor@vub.ac.be.

1. Introduction:

Cyclones are widely used for removing industrial dust from air or process gases. They are the most frequently encountered type of gas-solid separator in industry. The primary advantages of cyclones are economy, simplicity in construction and ability to operate at high temperature and pressures. The principle of cyclone separation is simple: the gas-dust mixture enters from the inlet section where the cylindrical body induces a spinning (swirl), vertical flow pattern to the gas–dust mixture. Centrifugal force separates the dust from the gas stream; the dust travels to the walls of the cylinder and down the conical section to the dust outlet. The gas exits through the vortex finder from the top.

A considerable amount of experimental data exists on cyclone performance, obtained for the most part in the 1930s and 1940s, using impact tubes, before the availability of Laser Doppler Anemometry (LDA) or hot-wire probes, which form the basis of many semi-empirical correlations on which current design practice is based. The design method usually depends on a number of expressions to obtain an overall pressure drop and a characteristic grade efficiency curve, as a function of geometrical factors and operating conditions [1].

This paper presents the results of flow simulations of the Stairmand cyclone using Reynolds stress model (RSM) and Large eddy simulation (LES) using the FLUENT finite volume solver. The computational results are compared to that obtained by different mathematical models. The axial and tangential velocity profiles are compared with the available experimental and computational results in the literatures. The flow field patterns are discussed in details. The DPM modeling used to calculate the collection efficiency (cut-off size) based on one-way coupling. The present study focuses on the effect of the used turbulence methodology on the estimated cyclone performance and the flow pattern, which is not well reported in previous literatures.

2. Cyclone Geometry and Solver Settings

The cyclone geometry and dimensions are given by Table 1 and Fig. 1, and are based on the high-efficiency Stairmand design. The inlet velocity equals 20 m/s corresponding to

0.08 m^3/s discharge, air density 1.225 kg/m^3 and dynamic viscosity 1.7894 E-4 Pa.s, which gives a Reynolds number of 2.8E5 based on the cyclone diameter and the area averaged air inlet velocity. The cyclone volume is 0.1976 m^3, resulting in an average residence time (cyclone volume/volume flow rate) of 0.247 s. The turbulence quantities were uniformly imposed at the inlet by using a turbulence intensity of 10%, and the characteristic turbulence length scale l_m=0.07 b where b is the inlet section width.

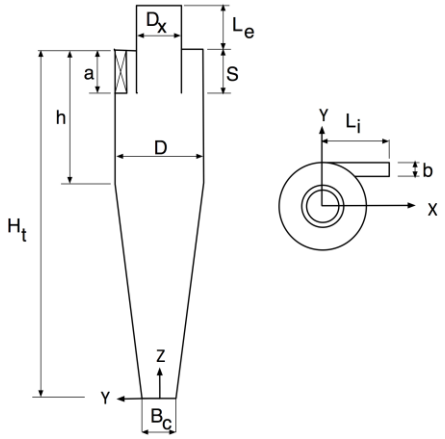

Figure (1): *Schematic diagram for cyclone separator*

Table (1): *The values of geometrical parameters (D=0.205 m)*

a/D	b/D	B_c/D	D_x/D	h/D	H_t/D	S/D	L_i/D	L_e/D
0.5	0.2	0.36	0.5	1.5	4	0.5	1.0	0.5

Table (2): *The locations of axial stations*

Section	S1	S2	S3	S4	S5	S6	S7	S8	S9	S10	S11	S12
z/D	0.85	1.0	1.53	1.73	1.87	2.75	2.9	3.19	3.5	3.75	4.25	4.5
z [m]	0.174	0.205	0.314	0.354	0.384	0.564	0.594	0.654	0.72	0.77	0.87	0.92

Grid refinement tests were conducted in order to make sure that the solution was not grid dependent. Three meshes are used for RSM simulations viz. around 65,000 cells, 250,000 cells and 497,000 hexahedral cells. There was no considerable difference in the velocity profiles (tangential and axial components) at different sections obtained on the last two meshes. The solution on the 250,000 cells mesh is therefore regarded as a grid independent solution. For the LES simulation a mesh of around one million hexahedral cells was used. Table 2 indicates the position of different locations used for the analysis of the flow field. Surfaces from S1 till S5 are located in the cone section. Surfaces from S6 till S8 are located in the cylindrical part below the vortex finder entrance. Surface S9 is located at the entrance of the vortex finder. Surface S10 is located at the middle of the entrance region. Surfaces S11 till S12 are located away from the cyclone body, in the vortex finder.

The SIMPLEC algorithm was used for pressure-velocity coupling, the QUICK scheme for spatial discretization and the PRESTO scheme for pressure discretization. The simulation is unsteady with a time step of 0.001s in case of RANS and 0.0001s for LES. The boundary condition at gas outlet is “outflow” boundary conditions, where all transport

variables have a zero normal gradient. This boundary condition is valid for fully developed flow, and this is the reason why the vortex finder is extended one-half cyclone diameter above the top of the cyclone in the present study to allow the exit flow to be fully developed [2]. The effect of this distance on the flow field has been the subject of different investigations e.g. [3,4] where this distance was varied between zero and four cyclone diameters. Wang et al. [4] investigated the effect of the outflow length on the flow field and velocity profile and suggested to have the gas outlet boundary condition at a distance longer than the cyclone radius. The bottom of the cyclone was closed and a wall boundary condition is applied (no dustbin included), in the literatures it is also reported that, the dustbin connected to the cyclone should be incorporated in the flow domain as it affects the results obtained, e.g. Xiang and Lee [2]. On the other hand numerous studies were performed without dustbin, e.g. Slack et al. [1], Wang et al. [4] with good matching with experimental results.

For the discrete phase modeling (DPM) a one-way coupling for RANS and LES simulation is used. The maximum number of time steps, N_{max}=1E6, which is the maximum number of time steps used to compute a single particle trajectory. In the current study the Rosin-Rammler size distribution is used. The complete range of sizes is divided into an adequate number of discrete intervals; each represented by a mean diameter for which trajectory calculations are performed. For the Rosin-Rammler size distribution, the mass fraction of particles of diameter greater than *d* is given by,

$$Y_d = e^{-\left(d/\bar{d}\right)^n} \tag{1}$$

Where *d* is the size constant (mean diameter) and *n* is the size distribution parameter (spread rate). The particle density is 860 kg/m^3, minimum particle diameter equals 5.0E-7 m, maximum diameter equals 1E-5 m, mean diameter equals 2.5E-6 m, and the spread rate equals 2.0 and number of particle diameters equals 10. Steady particle tracking used in the current study with assumed zero particle velocity at inlet. The particle mass flow rate equals 0.001 kg/m^3, corresponding to particle inlet concentration C_{in} (particle mass flow rate / gas flow rate) equals 0.013 kg/m^3.

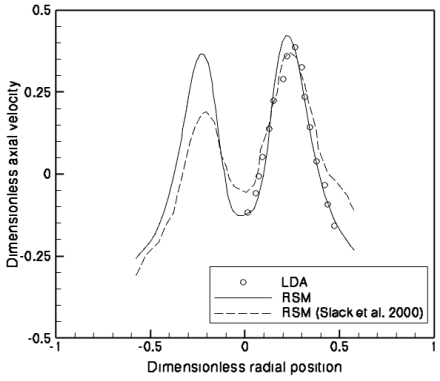

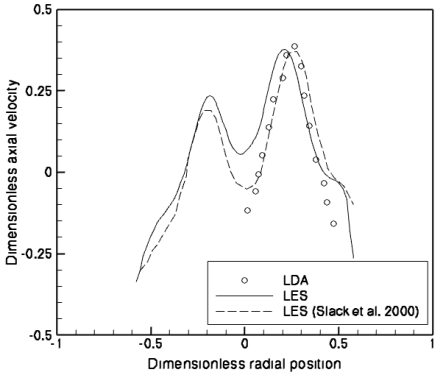

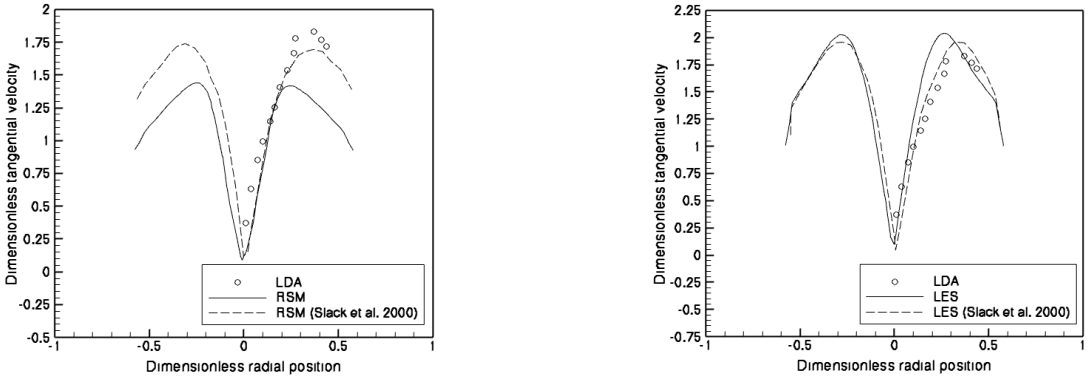

Figure (2): Comparison of the time averaged axial and tangential velocity profiles between measurements Boysan et al. [5], RSM and LES simulation from Slack et al. [1], and the current RSM and LES results at a section S1 where Z=174 mm from bottom. From left to right RSM and LES results. From top to bottom: axial velocity and tangential respectively.

3. Results:

3.1. Validation of results

In order to validate the obtained results, it is necessary to compare the prediction with experimental data. The comparison is performed with the aid of the measurements presented by Boysan et al. [5]. The velocity profiles presented in Boysan et al. [5] have been measured using a backscatter Laser Doppler Anemometry (LDA) system. Comparison was then made between the present simulation and the simulation results presented by Slack et al. [1] and the measured axial and tangential velocity profiles at axial stations S1 for both RSM and LES results. Figure 2 presents the comparison between the experimental and simulated results for the time averaged tangential and axial velocity components. The simulated axial velocity profile agree quiet well with the measurements especially for RSM results, and the current simulation (using 250000 cells) matching experimental results better than that of Slack et al. [1] (using 40000 cells) as a finer mesh was used in the current study. The same conclusion can be obtained from axial velocity profile for LES results.

Figure 2 shows a slight difference between the CFD results and experimental tangential velocity profile especially away from the cyclone center, while the matching is quite well near the cyclone center (the same conclusion obtained by other researchers, e.g. Xiang and Lee [2]). LES results for tangential velocity profile matches experimental results better than RSM results did. However only the results at section S1 are presented here, the results at other stations are quite similar. Considering the complexity of the turbulent swirling flow in the cyclones, the agreement between the simulations and measurements is considered to be quite acceptable.

3.2. Comparison of the RSM and LES Flow Patterns

Table 3 depicts some of the results produced in the current study. First, a comparison between the flow patterns obtained from Reynolds stress model and large eddy simulation at sections X=0, S2, S7, S10 and S12 for three flow variables, viz. the dimensionless time averaged static pressure $[p/(0.5*\rho*V_{in}^2)]$, tangential velocity $[v_t/V_{in}]$ and axial velocity $[v_a/V_{in}]$. The static pressure contour plots show that, the static pressure decreases radially from wall to center. A negative pressure zone appears in the forced vortex region (central

region) due to high swirling velocity. The pressure gradient is largest along the radial direction, while the gradient in axial direction is very limited. The cyclonic flow is not symmetrical as is clear from the shape of the low-pressure zone at the cyclone center (twisted cylinder). The shape of the pressure contours for RSM and LES are very similar but LES systematically predicts higher values. The central region of the cyclone is more twisted in case of LES.

Based on the contour plots of tangential velocity given by Table 3, and the velocity profile given by Table 4, the following comments can be drawn. The tangential velocity distributions for the two cases are nearly identical in pattern, with the highest velocity occurring in case of LES. The tangential velocity profile at any section is composed of two regions, one inner and one outer. In the inner region the flow rotates approximately like a solid body rotation (forced vortex), where the tangential velocity increases with radius. After reaching its peak the velocity decreases with radius in the outer part of the profile (free vortex). This profile is a so-called Rankine type vortex. The values of tangential velocity in LES are higher than RSM and match experimental values better than RSM results especially for the maximum tangential velocity. The position of maximum velocity is nearly the same for RSM and LES at each section. The axial velocity contours indicates there are two flow streams. A downward flow directed to the cyclone bottom (negative axial velocity), and an upward flow directed to the vortex finder exit. The axial velocity equals zero at the walls and is maximal close to the position of maximum tangential velocity. The axial velocity profiles shown in Table 4 exhibit a severe asymmetrical feature. Both the RSM and LES results match well the experimental results away from the central region. RSM results match better the experimental measurements in the central region.

3.3. Cut-off size and pressure drop

Figure 3 shows a comparison between the grade efficiency curves obtained from Reynolds stress model and large eddy simulation. Although the cut-off sizes obtained by the two methods are close, the shape of the two curves is quite different with the slope of the LES curve being much more steeper.

Table 4 depicts a comparison between the Euler number (dimensionless pressure drop) and the cut-off size obtained from RSM, LES and seven mathematical models, viz. (Barth model [6], the Muschelknautz method of modeling (MM)[7,8], Stairmand model [9], Casal and Martnez-Benet model [10] and Shepherd and Lapple model [11], Iozia and Leith model [12], Rietema model [13], for more detail refer to Hoffmann and Stein (2008) [14]). The Euler numbers estimated by different models are close to that of RSM except Barth model. While the cut-off size obtained by all methods all very close, except MM model which is over estimated.

4. Conclusions and future work:

Reynolds stress model and Large eddy simulation have been used to simulate the turbulent flow in the cyclone separator and estimation of pressure drop and cut-off size. Also seven mathematical models are used to estimate the performance.

The flow pattern obtained by both RSM and LES are close with more details obtained in case of LES. The static pressure and the tangential velocity are overestimated in case of LES. The axial velocity values are close in case of RSM and LES with local peak in the

central region inside the vortex finder. The tangential velocity profiles for LES match experimental profiles better than RSM especially in the free vortex part. The axial velocity profile in case of RSM matches better the experimental especially in the forced vortex part. The Euler numbers estimated by different models are close to that of RSM except Barth model. The cut-off sizes obtained by all methods are very close, except MM model, which is over estimated.

Both RSM and LES predict well the main features of the cyclonic flow, with the benefit of more flow details in case of LES and ability to capture unsteady phenomena of the high swirling flow like vortex core precession. LES is favorable in case of transitional flow, like the case of small (sampling) cyclone. While LES is computationally cost. Away from that, RSM is enough with good matching with experimental measurements. As extension to this study, Detached eddy simulation (DES) results to be compared with RSM and LES. Also a comparison between one-way and two-way coupling for discrete phase modeling is a possible extension.

Table (3): *The time-averaged contour plots for CFD simulations using RSM and LES*

	RSM	LES
The static pressure [-]	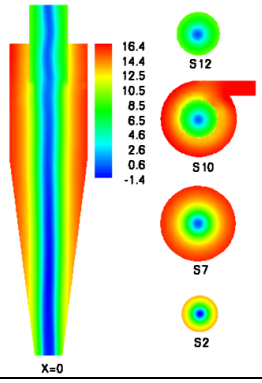	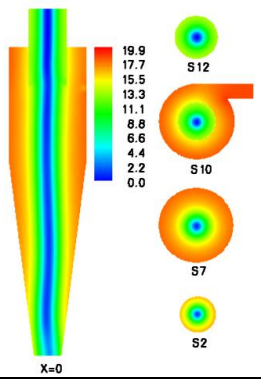
The tangential velocity [-]	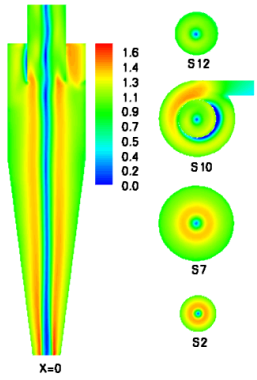	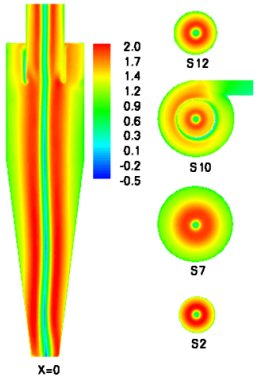
The axial velocity [-]	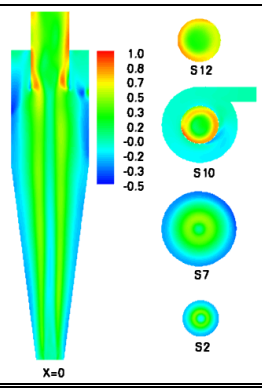	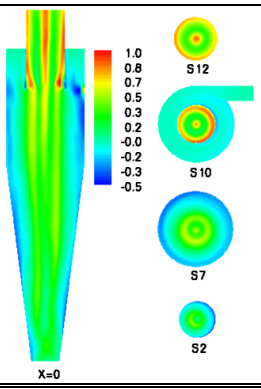

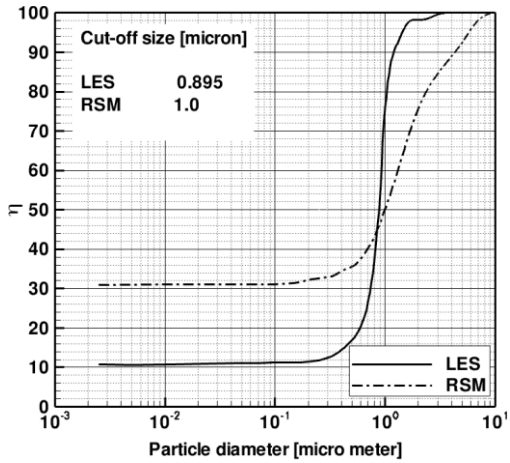

Figure (3): Grade efficiency curves for RSM and LES.

Table (4): *The time-averaged velocity profiles for CFD simulations using RSM and LES at the first five sections.*

Section	Tangential velocity	Axial velocity
S1	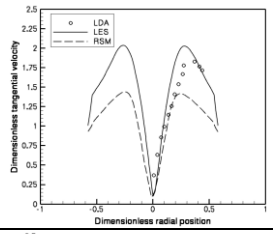	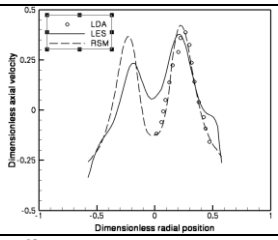
S2	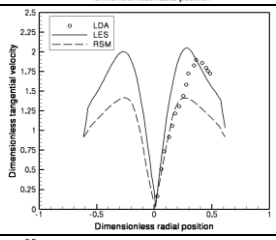	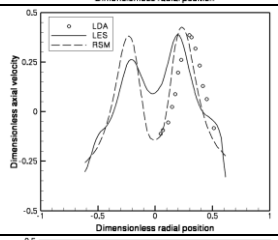
S3	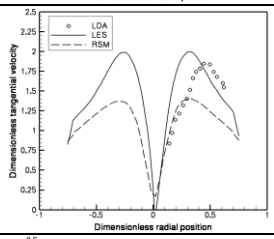	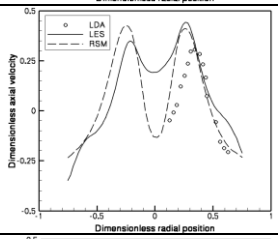
S4	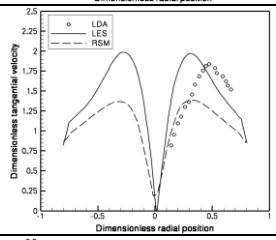	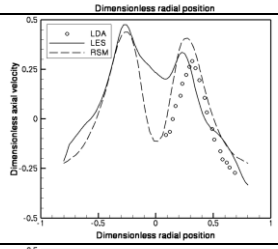
S5	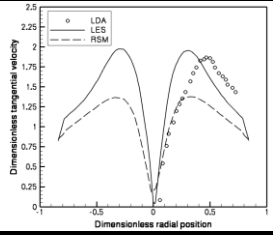	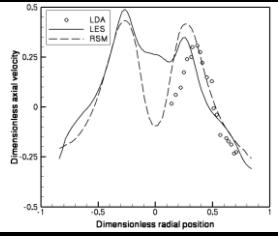

Table (5): *The cyclone performance parameters using RSM, LES and different seven mathematical models*

	RSM	LES	Barth	MM	Stairmand	Sphered	Casal	Iozia	Ritema
Euler number [$\Delta p/(0.5*\rho*V^2_{in})$]	4.216	7.497	8.03	5.07	6.84	6.4	5.14	-	-
Cut-off size [micron]	1.00	0.895	1.05	2.04	-	-	-	0.987	0.903

References:

[1] M. D. Slack, R. O. Prasad, A. Bakker and F. Boysan, *Advances in cyclone modeling using unstructured grids*. Trans IChemE. Vol. 78 Part A, P 1098-1104, November 2000.

[2] R. B. Xiang, K. W. Lee, *Numerical study of flow field in cyclones of different height*. Chemical Engineering and Processing, Vol. 44, P 877-883, 2005.

[3] St. Schmidt, H. M. Blackburn and M. Rudman, *Impact of outlet boundary conditions on the flow properties within cyclone*, 15th Australasian Fluid Mechanics Conference. The University of Sydney, Sydney, Australia, 2004.

[4] B. Wang, D. L. Xu, K. W. Chu, A. B. Yu, *Numerical study of gas solid flow in a cyclone separator*, Applied Mathematical Modeling, Vol. 30, P 1326-1342, 2006

[5] F. Boysan, B. C. R. Ewan, J. Swithenbank and W. H. Ayers, *Experimental and theoretical studies of cyclone separator aerodynamics*. IChemE Symp Series Vol. 69, P 305 – 320, 1983.

[6] W. Barth, *Design and layout of the cyclone separator on the basis of new investigations*, Brennstoff-Warme-Kraft, Vol. 8, No. 4, P 1–9, 1956.

[7] E. Muschelknautz and M. Trefz, *Design and calculation of higher and design and calculation of higher and highest loaded gas cyclones*, Proceedings of Second World Congress on Particle Technology, P 52–71, October 1990.

[8] E. Muschelknautz and M. Trefz , *VDI-Wärmeatlas*. VDI-Verlag Dusseldorf, 6 Auflage, Lj1 – Lj9, 1991.

[9] C. J. Stairmand, *Pressure in cyclone separator*, Engineering, Vol. 168, P 409–412, 1949.

[10] J. Casal and J. M. Martnez-Benet, *A better way to calculate cyclone pressure drop.* Chemical Engineering, Vol. 90, No. 2, P 99–100, 1983.

[11] C. B. Shepherd, and C. E. Lapple, *Flow pattern and pressure drop in cyclone dust collectors cyclone without inlet vane*. Industrial & Engineering Chemistry, Vol. 32, No. 9, P 1246–1248, 1940.

[12] D. L. Iozia, D. Leith, *The Logistic Function and Cyclone Fractional Efficiency,* Journal of Aerosol Science and Technology, Vol. 12, P 598−606, 1990.

[13] K. Rietema, *Het mechanisme van de afscheiding van fijnverdeelde stoffen in cyclonen* (in Dutch), De Ingenieur, Vol. 71, No. 39, ch59–ch65, 1959.

[14] A. C. Hoffmann, and L. E. Stein, *Gas Cyclones and Swirl Tubes Principle, Design and Operation*, 2nd Edition, Springer, 2008.